NEW DEVELOPMENTS IN THE DETERMINATION OF THE STRUCTURE OF COMPLEX ORGANIC MOLECULES

W. HOPPE

[in collaboration with N. BRODHERR, HP. ENGLMEIER, J. GAßMANN, A. GIEREN, S. HECHTFISCHER, L. PREUß, M. RÖHRL, J. SCHAEFFER, E. SCHMIDT, W. STEIGEMANN and K. ZECHMEISTER]

Abteilung für Röntgenstrukturforschung am Max-Planck-Institut für Eiweiß- und Lederforschung, München und Physikalisch-Chemisches Institut der Technischen Hochschule, München, Abteilung für Strukturforschung

INTRODUCTION

There can be no doubt that nowadays determinations of the structure of organic molecules can only be carried out economically, when automatic single crystal diffractometers are used. Such a machine collects more data in a fortnight than a hardworking man in many months. But it is not only the speed and the convenience, but also the inherent accuracy of the measurement which counts. Several diffractometers of different type and construction are available and some laboratories have already gained considerable experience in using them. I do not intend to discuss the different principles; my paper will be restricted to the most general instrument, i.e. to the four-circle diffractometer. This instrument permits the measurement of the full three-dimensional array of reflections with one crystal setting. If desired, the measurements can even be made on an unoriented crystal. My report will concentrate on our experience with these instruments over the last few years.

FOUR CIRCLE DIFFRACTOMETER

Two important factors to be considered in designing a diffractometer are the distances between the focus of the x-ray tube and the crystal, and between crystal and counter aperture. The factors which influence the choice of these distances are different for photographic work and diffractometer work. In photographic work the peak intensity of the spot is most important. Its size has little influence on the accuracy of a density measurement. In diffractometer work, however, it is simply the number of counts, which limits the basic (statistical) accuracy.

In *Figure 1* the basic relations are explained. The square represents the focus of the tube as seen from the crystal. At any particular angle within the ϑ reflection range, a narrow rectangular area inside the focus contributes to the intensity (hatched rectangle in *Figure 1*). This rectangle is the section of the lattice plane reflection cone with the focus; it is, therefore, slightly curved. Its breadth depends on the mosaic spread and the size of the crystal

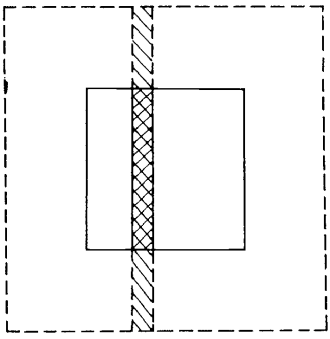

Figure 1. Scanning of the focus by the reflecting crystal

and on the chromatic spread of the radiation spectrum. The best intensity output will be achieved if the collimating system is constructed in such a way that every point of the crystal can 'see' every point of the focus. Thus the direction and divergence of the primary beam will be determined by the geometry of the focus and the crystal. On the other hand, the collimator opening should not be larger than necessary in order to avoid unwanted radiation. The entrace collimator, in particular, should be matched to the focus and placed as close as possible to the tube window in order to cut out radiation not coming from the focus.

Let us now halve the focus to crystal distance. This means that to the crystal the focus will appear larger than before. The virtually magnified focus is represented in *Figure 1* by the dashed square. The intensity at a given angle within the ϑ range will now be doubled because the section of the reflection cone with the virtual focus will be twice as long. It should be mentioned that the effective breadth of the rectangle will also change; but this does not matter as long as the rectangle is narrower than the image of the focus. If one scans through the ϑ range with the same angular velocity in both cases, one obtains the four-fold intensity in case two. On the other hand the reflection curve becomes approximately twice as broad. This means that one need spend only half the time on the measurement. But the real intensity gain is somewhat better than two because the factor for the effective broadening is somewhat less than two for reasons which we will not discuss here. The intensity gain is associated with a loss of resolution. This means that one has to match the focus-to-crystal distance to the unit cell size. The important point is that this ideal distance is surprisingly small even in the case of quite complicated organic structures and of copper radiation. Our efforts to minimize this distance have led us to an asymmetric design with the primary beam as reference beam and with an open Eulerian cradle. The asymmetry permits us to make the cradle stable enough in spite of the space taken up by the tube, and the open cradle allows free access to all 2ϑ-regions. The last point is of importance as the head of the tube comes nearer to the crystal and tends to obstruct the counter. If a higher resolution is required, it is much better to use a fine focus x-ray tube with its higher specific loading than to increase the focus to crystal distance. Automatic diffractometers are expensive instruments and should be used

economically. It is, therefore, a little surprising how little effort has been devoted to optimizing the intensity output; the working distances in existing diffractometers vary by more than 1:2!

Another important parameter is the crystal-to-counter distance. Again applying simple geometric considerations, it can be shown that this distance should be made as long as possible (especially for bigger crystals) in order to reduce the continuous background[1]. Evacuated or helium-filled beam tunnels are necessary to reduce air absorption. With monochromators—e.g. with the recently developed graphite monochromators—the white radiation background can be completely removed. But the background produced by thermal diffuse scattering of higher order and by scattering of the crystal support will not be reduced. Therefore, long beam tunnels may remain useful especially for the measurement of weak high order reflections.

I do not intend to discuss diffractometer principles in detail, as this was the substance of a lecture given elsewhere some weeks ago[2]. I shall restrict myself to some comments concerning the use of the diffractometer. But I should like to stress that the stability and accuracy of an instrument—which allows precise structures to be measured in a routine way—is not only important for theoretical chemistry but also for the x-ray analysis of chemical constitution. It facilitates the determination of the chemical formula.

It is advisable to check the crystal first by photographic means. Superstructure, disorder, splitting of reflections etc. will thus be immediately recognized. Good intensity measurements require good crystals. Our self-check devices proved to be very useful. *Figure 2* shows the curves of four reflections of beryllium acetate for values of ϑ up to about 50°. In the five-point measuring routine, the left-hand-side of a profile is compared with the right-hand-side in order to check the centering of the reflection curve. *Figure 2* shows the quotient of the half integrals for reflections off-centre by various amounts. The figure shows the striking sensitivity of this criterion. It can be recognized that the quotient 1·0 represents fairly accurately a centred reflection curve. This check recognizes errors in the lattice spacings due to incorrect determination of lattice constants. When applying this test one should not forget that absorption also shifts the reflections. The programmed half-screens in the counter aperture (*Figure 3*) check whether the spot lies in the middle of the aperture. Contrary to the five-point measuring routine, this test requires additional measuring time. It should, therefore, only be made on a selected set of reflections. Half-shutter measurements on reference reflections allow the slightest misorientation of the crystal to be recognized.

I mentioned that the primary beam is taken as the reference for the zero position in our diffractometer. The correct way to adjust the zero is to replace the crystal by a small pinhole. This pinhole acts as a camera obscura which produces an image of the focus in the counter. Scanning of this focus with a slit in the counter aperture has the same effect as measuring the zero reflection curve of an ideal absorption-free small crystal. The maximum in this scanning curve is the zero point. Stray radiation does not affect the relative shape of the profile. It is, however, advisable to make this measurement using a low voltage in the x-ray tube (in the neighbourhood of 10 kV for copper radiation). The metal foil filters which are necessary to reduce

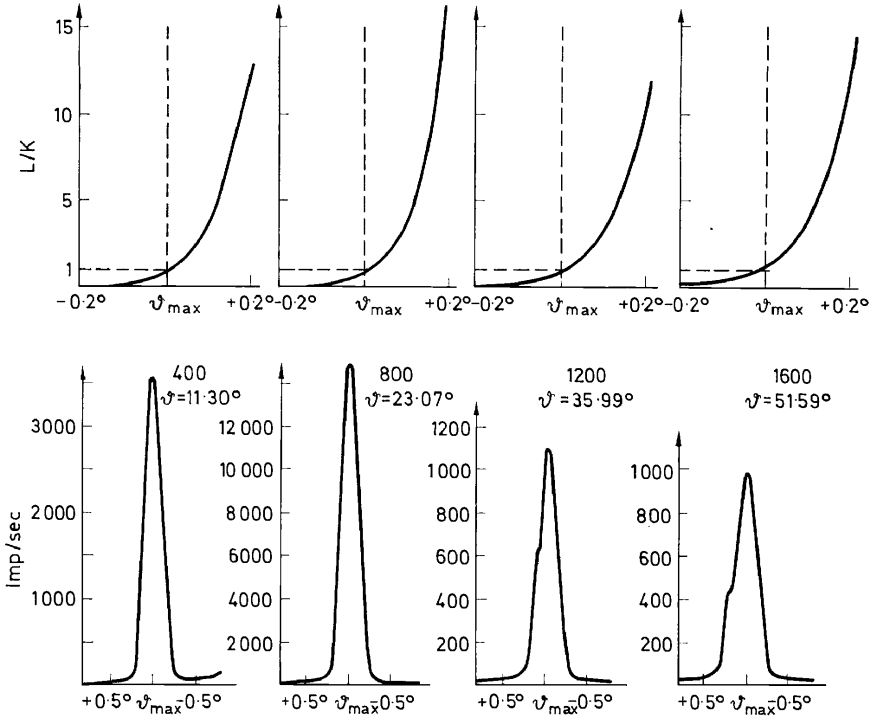

Figure 2. Lower diagrams: Reflection scans. Upper diagrams: Quotient of half integrals for these reflections when off-centred by varying amounts in θ

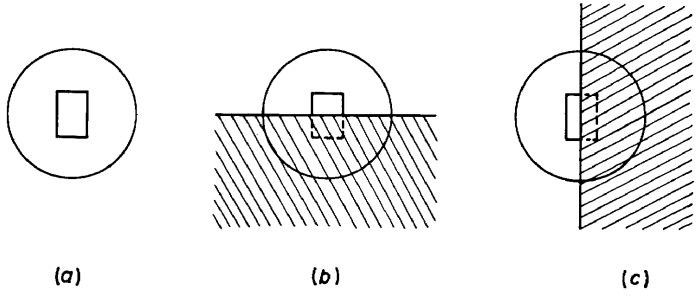

Figure 3. Programmed half-shutters (*a*) open aperture, centred reflection; (*b*) lower half of the reflection shadowed off; (*c*) right-hand-side of the reflection shadowed off

the primary intensity allow only the short wave components to pass through. If their wavelengths deviate too much from the wavelength of the characteristic radiation, their intensity profiles within the focus can differ due to the different absorption of the radiation in the anode. Another often-used procedure is to measure the reflection curve of a lattice plane at ϑ and at $-\vartheta$. The symmetry line then represents the zero direction.

I should now like to stress the importance of absorption corrections even for weakly absorbing crystals. The shape factor of the absorption is especially

dangerous. The necessary correction can however be calculated. An experimental procedure which takes into account not only the shape of the crystal but also the absorption in the material surrounding it, etc. has been worked out recently[3]. This procedure is now used in our laboratory as a matter of routine.

Closed cradle installations and a quarter-circle cradle installation with crystal inverter[2] allow the measurement of the whole reciprocal sphere. But obstruction and shadowing-off of the cradle in the case of a full circle instrument and of the crystal support substantially reduce the access to reflections outside the quarter-circle region. If the crystals have been mounted on a glass fibre, additional absorption in this fibre occurs for the accessible reflections as well. It is, therefore, advisable even for the users of a closed circle instrument to organize the measurements in such a way that they can be carried out in quarter-circle geometry. It is well known that this can be achieved even for the measurement of anomalous scattering for all space groups with the exception of P_1 if the orientation has been properly chosen. Measurement of anomalous scattering needs an especially careful absorption correction. Sometimes it is claimed that this correction is not so important if one measures the Bijvoet pairs $I\ (h, k, l)$, $I\ (\bar{h}, \bar{k}, \bar{l})$ as both measurements are influenced by the same absorption factor. But this is only true for crystals with centro-symmetrical shape and no absorption in the surrounding material. Our experience has shown that even the small intensity changes introduced by bromine as an anomalous scatterer allow the determination of the absolute configuration of quite complicated organic structures if the absorption has been properly corrected.

One attraction of a diffractometer coupled with a computer is that it can measure the reflections of an unoriented crystal. First, the orientation of the crystal or even the whole lattice geometry of an entirely unknown crystal are determined. Second, the computer calculates all reflection angles and controls the measurements. The difficulty in this scheme is that the important photographic check of the crystal would not be easy to undertake. One could provide film holders for the diffractometer, but this would be a misuse of the diffractometer. Cheap precession- and Weissenberg-goniometers can do this job very much better; during the photographic work the diffractometer can be used for other problems.

The fascinating aspect of measurements on unoriented crystals is that a scientist without special crystallographic training or even a member of the technical staff could make crystallographic measurements. The necessary photographic work could be included in an economical way if one translates all manipulations of the crystallographer into the language of photographic cameras. The following procedure could cover all aspects:

1. Determination by diffractometer of the orientation (and eventually lattice geometry) of a crystal arbitrarily mounted on a goniometer head with arcs set to zero.
2. Computation of the angles which should be set on the arcs on the goniometer head in order to bring the crystal into a convenient orientation.
3. Setting of the arcs and transfer of the goniometer head with crystal to a camera. Photography of several reciprocal lattice planes.
4. Calculation of the geometry of the diagrams in the computer and

comparison of calculated and photographed diagrams in order to judge the suitability of the crystal for intensity work.

5. Transfer of the crystal from the camera back to the diffractometer, determination of any small mis-orientation due to a non-precise hand-setting of the arcs and to the double transfer, measurement of all reflections with appropriate checks.

It is an advantage of this scheme that in many cases the measurement of anomalous scattering could also be carried out in the favourable quarter circle geometry. It is easy to generalize this scheme for special cases, where additional orders given by the computer (e.g. for remounting a closed circle diffractometer from the bisecting positions to the parallel position or for operations on the crystal inverter in a quarter circle installation) will be needed.

A further remark concerns the influence of thermal diffuse scattering on the accuracy of intensity measurements. Especially the one-phonon scattering is annoying as it peaks in the neighbourhood of the reflections. Thus the contribution of thermal diffuse scattering to the intensity measurement will depend on the divergence of the primary beam and of the counter[4]. It can easily be shown that this error will influence mainly the vibrational parameters of a crystal structure analysis. An accurate correction would require the determination of elastic constants, e.g. with measurements of diffuse scattering. The calculation of the corrections is possible only when all geometrical factors (divergence of primary beam, crystal size, mosaic spread, etc.) are known. Very accurate structure determinations also require corrections for primary and secondary extinction. Lately, new methods for the determination of these parameters have been introduced[5].

STRUCTURES AND METHODS OF STRUCTURE DETERMINATION

It has been shown above that even measurements for quite accurate structure determinations can be almost fully automated. In the last consequence, a system is possible where a sophisticatedly programmed computer in turn 'programs' the worker who will act under supervision of the computer and be checked by the computer. Has this trend to automation its counterpart in the theoretical methods for structure determination? It has. Already efficient crystallographic laboratories arrange their programs in a monitor system. Operations, which used to be done by the worker—search for peaks, drawing of Fouriers and of molecular models—have been transferred to the computer. Heavy-atom phasing can be done with programs which determine the heavy atom position in the Patterson map[6]. Using appropriate programs, phase determination with the convolution molecule method[7] or with direct methods can be done in a routine manner. Even the cumbersome step from the first tentative model to the structure by iterative (and intuitive) Fourier refinement is now being replaced by new computer methods (phase correction[8]) and computer controlled Fourier refinement[9].

In our laboratory we are working on organic structures with ring-systems of different kinds. During the discussion of some of our results, I shall show how new methods facilitated determinations of structure.

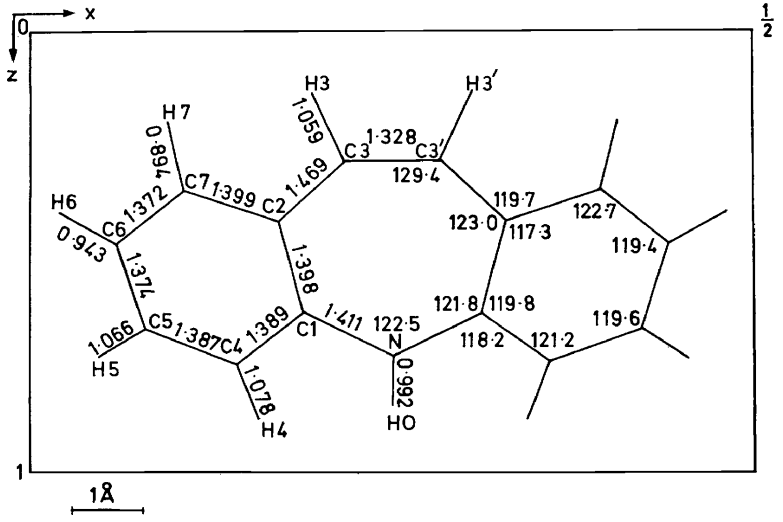

Figure 4. Dibenz[*b*,*f*]azepine: Projection of the molecule along *b*; bond lengths are given in left half, bond angles in right half of the molecule

Figure 4 shows the structure of the relatively simple heavy-atom-free organic molecule, dibenz[*b*,*f*]azepine $C_{14}H_{11}N$ (I). Several years ago, this structure was solved in projections by the convolution molecule method[10]

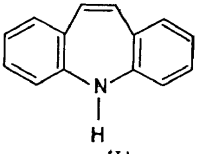

(I)

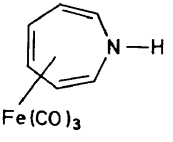

(II)

and has recently been refined using three-dimensional diffractometer data. Space group Pmnb, $a = 20{\cdot}46$ Å, $b = 8{\cdot}24$ Å, $c = 6{\cdot}05$ Å, $Z = 4$. The molecule is halved by a crystallographic mirror plane. *Figure 4* shows the projection along the *b*-axis with bond lengths ($R = 4{\cdot}7$ per cent, 741 reflections). *Figure 5* demonstrates the accuracy of the measurement—all hydrogen atoms in this three-dimensional difference Fourier synthesis show equal weights and are nearly spherical. The azepine ring does not obey the Hückel rule and should, therefore, be non-planar. *Figure 6* shows a molecule projected down the *z*-axis, where the boat conformation of the azepine ring is clearly recognizable. The nitrogen–hydrogen bond is bent out of the plane of sp^2-hybridization by an angle of approx. 40°. It is interesting that it has as yet not been possible to synthesize the unsubstituted azepine ring. But it exists in the complex azepine–iron–tricarbonyl $C_6H_7NFe(CO)_3$ (II); space group Pbca, $a = 12{\cdot}59$ Å, $b = 24{\cdot}08$ Å, $c = 12{\cdot}67$ Å. The heavy atom structure analysis was somewhat complicated by the fact that the structure contains two molecules in the asymmetric unit ($Z = 16$). Having solved the structure using photographic data[11], we collected 5637 reflections (only 2771 of them statistically significant) on our diffractometer using

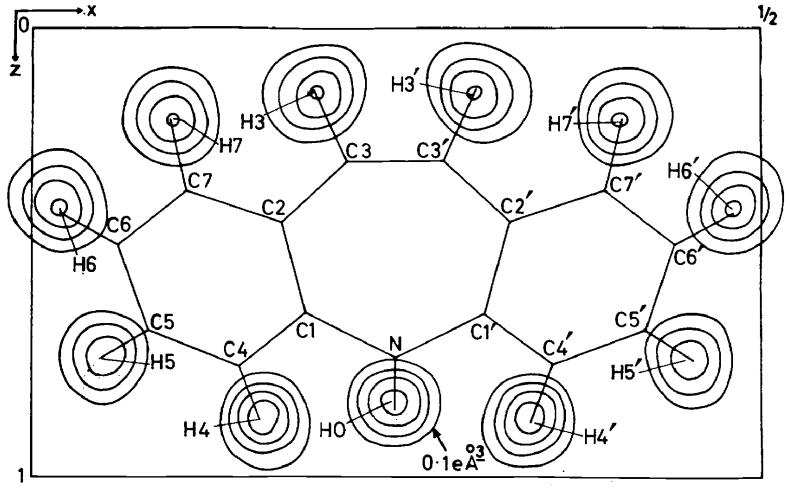

Figure 5. Dibenz[*b*,*f*]azepine: Difference Fourier synthesis showing hydrogen atoms (hydrogen atoms omitted from F_c); Contours are at intervals of 0·1 eÅ^{-3}, beginning with 0·1 eÅ^{-3}

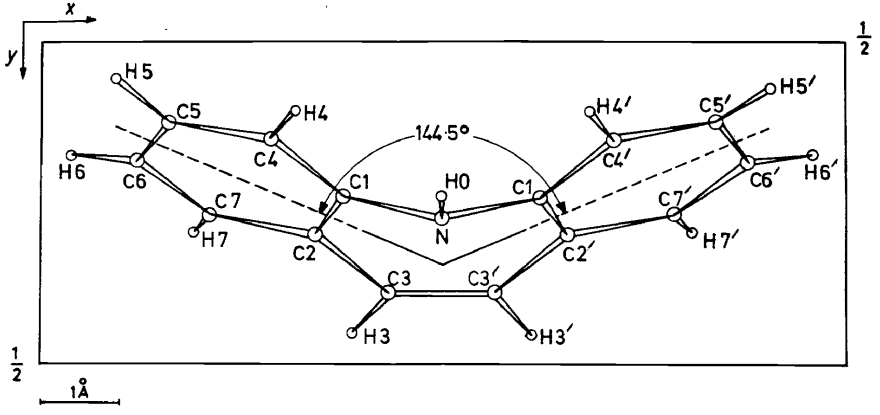

Figure 6. Dibenz[*b*,*f*]azepine: Projection of the molecule along *c*; the angle between the planes containing the benzene rings is indicated

molybdenum radiation. Careful absorption corrections were applied (R = 6·3 per cent). *Figure 7* shows the structure (without hydrogen atoms) projected along *a*. *Figure 8* shows the two molecules in the asymmetric unit with their bond-lengths. The interesting point is that the conformation of the azepine ring is different from that in dibenzazepine. The iron atom is bound to a planar butadiene system in the azepine ring. The complete azepine ring consists of two planes with a dihedral angle of 37°. More than 1 molecule in an asymmetric unit makes a structure determination more complicated, as more parameters have to be determined. On the other hand, a comparison of both molecules can give—at least in the case of rigid systems—an objective measure of the accuracy. The agreement

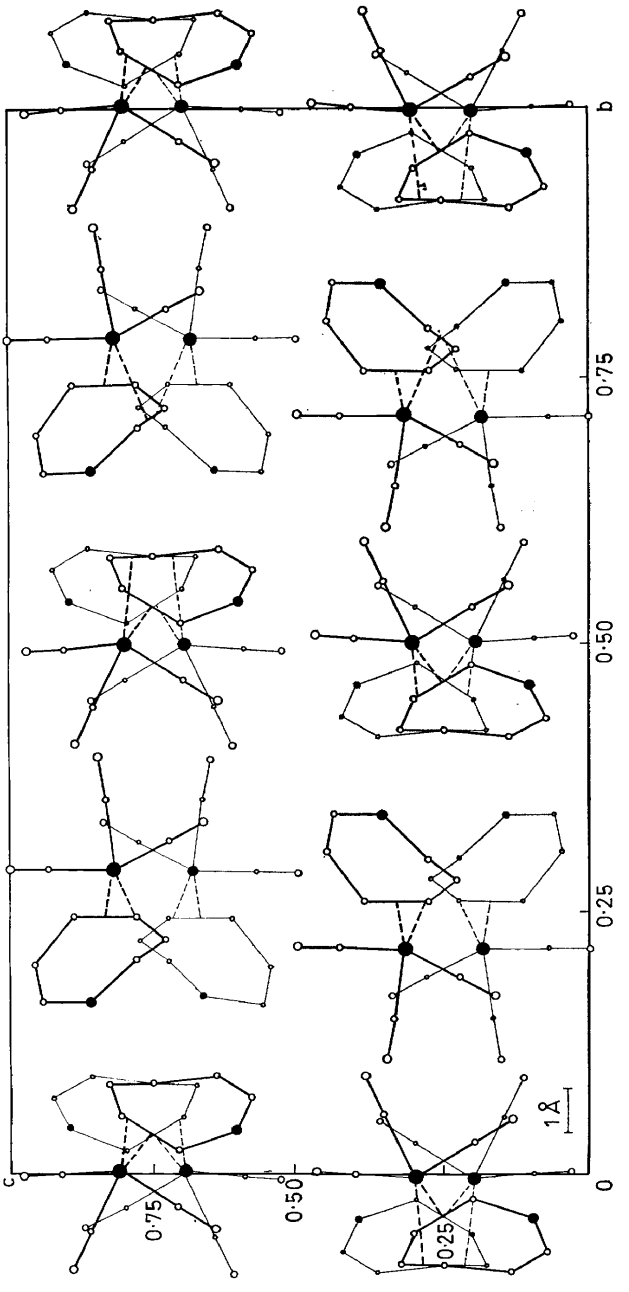

Figure 7. Azepine–iron–tricarbonyl. Projection of the crystal structure along *a*

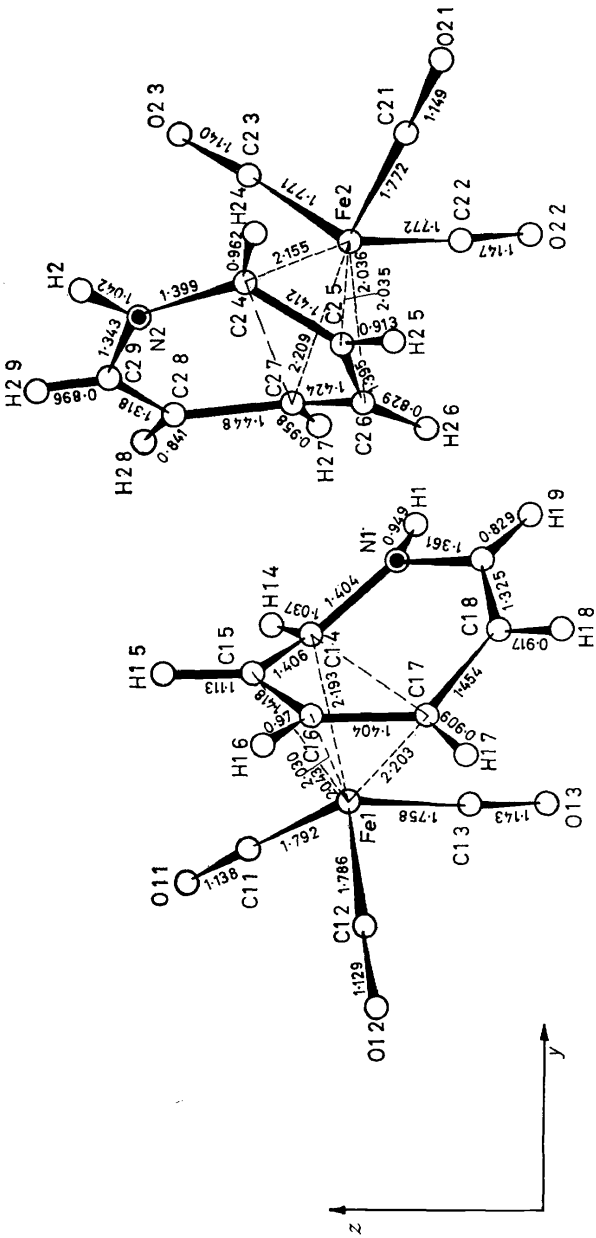

Figure 8. Azepine–iron–tricarbonyl. The two molecules of the asymmetric unit; the bond lengths are indicated.

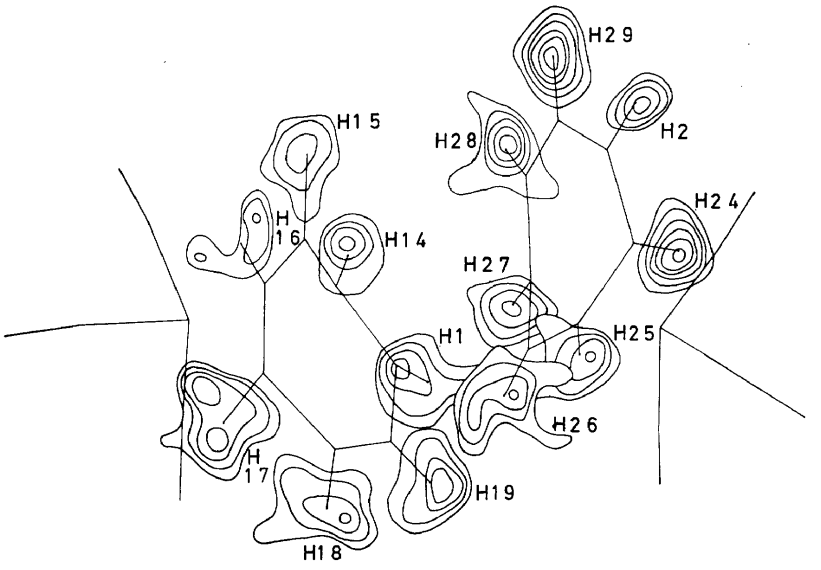

Figure 9. Azepine–iron–tricarbonyl. Difference Fourier synthesis (hydrogen atoms not included in F_c); contours are at intervals of 0·1 eÅ^{-3} starting with 0·2 eÅ^{-3}

between the two azepine rings in *Figure 8* is quite good; deductions from the bond lengths, therefore, are highly significant. The hydrogen atoms have been determined in both molecules (*Figure 9*), their positions being somewhat more influenced by errors than in *Figure 5*. The main structural features are, however, clearly shown. The iron–butadiene bond can be explained in a more classical way as a π-complex[12] bond or as a Diels–Alder-type addition[13] of iron to the butadiene system. A careful discussion of bond lengths, bond angles and hydrogen conformation indicates an intermediate state between the two possible models. Recently, our results on azepine have been confirmed by determination of the structure of other azepine compounds[14].

The next example again concerns the three-dimensional refinement of a structure which was solved in our laboratory some time ago. A structure analysis of 2,3,6,7-tetramethylnaphthazarine $C_{14}H_{14}O_4$ (III)[15] had shown

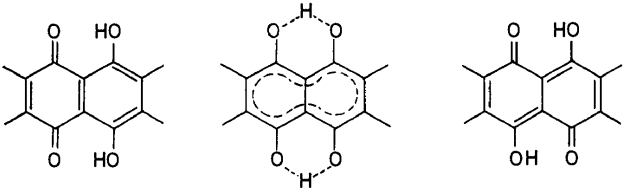

(IIIa) (IIIb) (IIIc)

that the molecules are situated on crystallographic centres of symmetry. A three-dimensional Fourier synthesis with photographic data[16] had shown that there was no additional mirror plane perpendicular to the molecular

plane. Thus, a statistical structure consisting of the unsymmetrical molecules (IIIa) of the usual chemical formulation was impossible. Also a highly symmetric system with symmetrical hydrogen bonds corresponding to formula (IIIb) could be excluded. Only the centrosymmetric formula (IIIc) was possible. Later, the structures of several crystal modifications of naphthazarine have been studied which confirm the centrosymmetric structure[17]. The substance crystallizes in Ibam $a = 17{\cdot}36$ Å, $b = 9{\cdot}94$ Å, $c = 6{\cdot}71$ Å. The molecule lies in the crystallographic mirror plane and half of it forms the asymmetric unit. *Figure 10* shows the structure; the molecules are in the plane $z = 0$ and (dashed) in the plane $z = 0{\cdot}5$. *Figure 11* shows

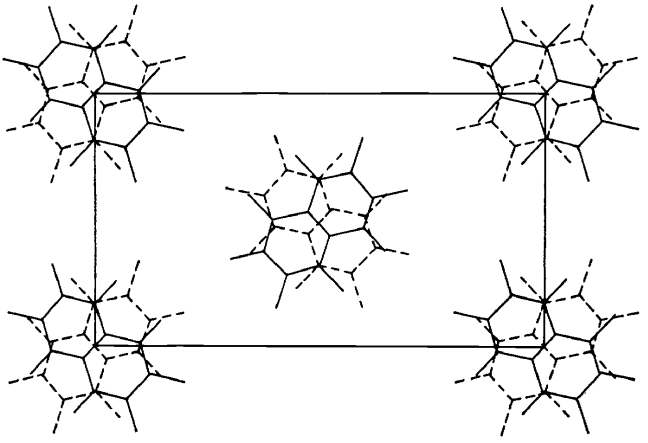

Figure 10. Tetramethylnaphthazarine. Projection of the crystal structure along *c*

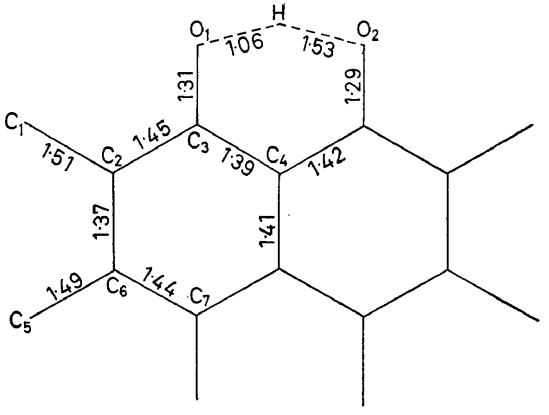

Figure 11. Tetramethylnaphthazarine. Molecular structure with bond lengths

the interatomic distances, and *Figure 12* the three-dimensional Fourier synthesis of the hydrogen atoms. As the hydrogen atoms of the methyl group C_1 have no mirror equivalents, the correct space group is Iba2, and there is no longer a restriction for the *z*-parameter of the carbon and oxygen atoms.

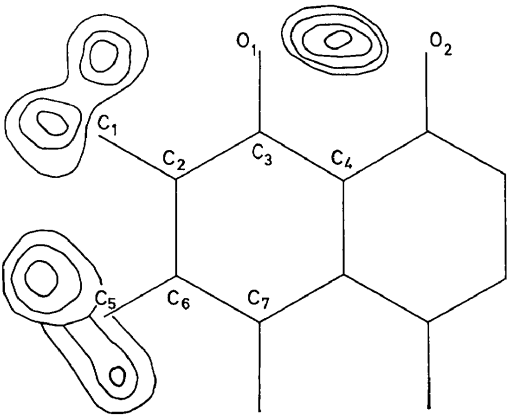

Figure 12. Tetramethylnaphthazarine. Difference Fourier synthesis (hydrogen atoms not included in F_c). *See 'Note added in proof' on* p. 488.

Another interesting example of a hydrogen bond configuration has been found in the structure of crystals of γ-rhodomycinone $C_{20}H_{18}O_7$ (IV). This

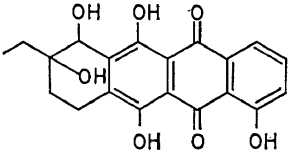

(IV)

substance belongs to the anthracyclinones, which have been studied by H. Brockman *et al.*[18]. The substance crystallizes in the space group $P2_1$, $a = 9{\cdot}193$ Å, $b = 29{\cdot}530$ Å, $c = 5{\cdot}994$ Å, $\beta = 98{\cdot}89°$ with two molecules in the asymmetric unit. *Figure 13* shows the structure in the (001)-projection,

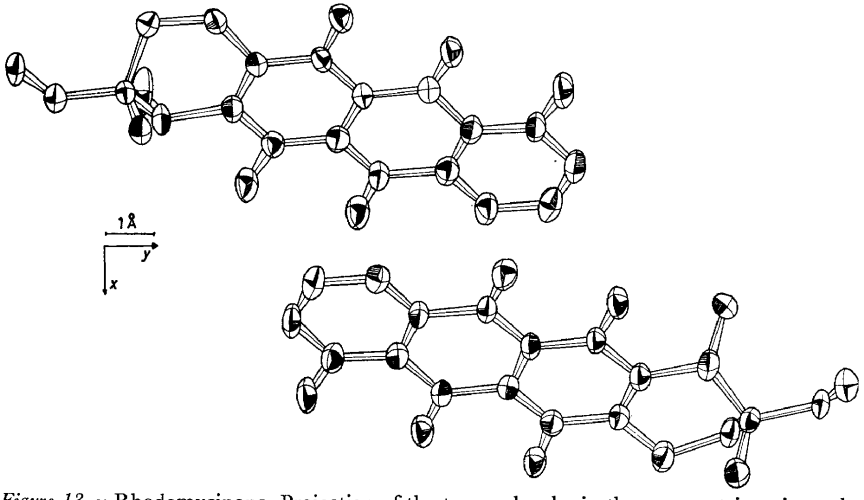

Figure 13. γ-Rhodomycinone. Projection of the two molecules in the asymmetric unit on the *a,b*-plane. The ellipsoids indicate the thermal vibrations of the atoms

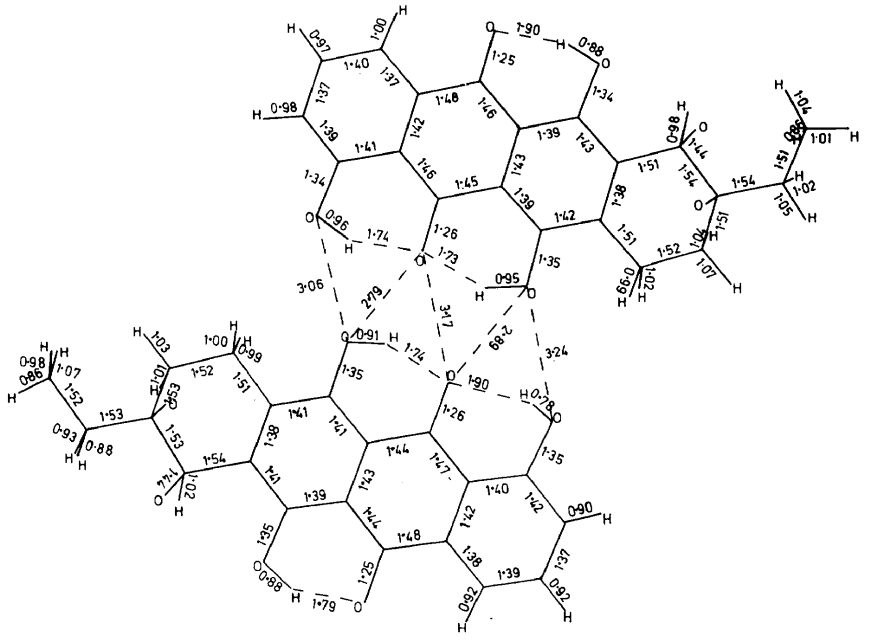

Figure 14. γ-Rhodomycinone. Projection of two molecules on the plane (201); bond lengths and important intermolecular distances are indicated

and *Figure 14* that in the (201)-projection. It can be seen from *Figure 14* that the two molecules in the asymmetric unit form a type of dimer, bound together by hydrogen bonds. The chinone group of the anthrachinone system is the acceptor for two intramolecular hydrogen bonds from the neighbouring hydroxyl groups. The configuration of the hydrogen bonds is very nearly the same as for the equivalent system in tetramethylnaphthazarine. On the other hand, the distances between adjacent oxygen atoms of different molecules indicate appreciable intermolecular interactions. This complicated system of bifurcated hydrogen bonds can be treated theoretically only if the positions of the hydrogen atoms are known. Again we see that the high accuracy of a diffractometer structure determination and thus the possibility of locating the hydrogen atoms can to some extent replace the localization of hydrogens by neutron scattering.

This can also be demonstrated in the next two structure determinations of bicyclo[2.2.2]octadiene-(2,5)-dicarboxylic acid(2,3) $C_{10}H_{10}O_4$ (V) and bicyclo[2.2.1]heptadiene-(2,5)dicarboxylic acid (2,3) $C_9H_8O_4$ (VI)[19]. The

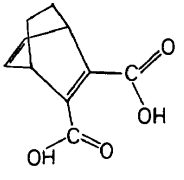

(V)

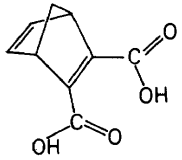

(VI)

first compound crystallizes in $P2_1/a$, $a = 16{\cdot}02$ Å, $b = 15{\cdot}27$ Å, $c = 7{\cdot}72$ Å, $\beta = 107{\cdot}01°$ with two molecules in the asymmetric unit. 2552 reflections (CuK_α) were measured. After an isotropic refinement (hydrogen atoms not included), the R-factor dropped from 13·5 to 8·8 per cent. Upon including the hydrogen atoms (found by a difference Fourier synthesis) a final R-factor of 5·0 per cent was achieved. *Figure 15* demonstrates how

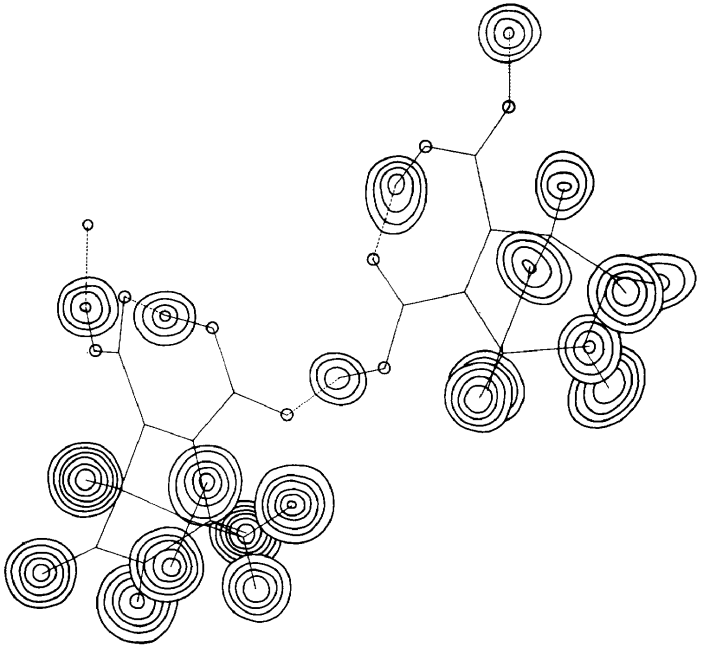

Figure 15. Bicyclo [2.2.2] octadiene (2,5) dicarboxylic acid (2,3). Difference Fourier synthesis (hydrogen atoms not included in F_c); contours are at intervals of 0·1 eÅ^{-3} starting with 0·1 eÅ^{-3}

beautifully the hydrogen atoms show up in this structure with 28 light atoms. It should be mentioned that only one set of diffractometer measurements was used, that no scaling of subsets (e.g. layer lines) has been carried out and that no special weighting scheme (apart from some extinction corrections) has been applied. *Figure 16* shows the interatomic distances. The good agreement of equivalent bond lengths is immediately apparent.

The structure of bicyclo[2.2.1]heptadiene(2,5)dicarboxylic acid(2,3)[17] turned out to be statistical. The compound crystallizes in $Pna2_1$ (the statistical structure in Pnam) with $a = 16{\cdot}48$ Å, $b = 7{\cdot}72$ Å, $c = 6{\cdot}44$ Å and one molecule in the asymmetric unit. *Figure 17* shows two translationally equivalent molecules bound together by intermolecular hydrogen bond similar to that shown in *Figure 16*. The maleic acid system lies in a crystallographic mirror plane; this means that the C-atoms 5,8,9 will be statistically doubled by this plane. Therefore, the bond lengths involving these atoms cannot be determined accurately. This can well be seen in *Figure 17*. On

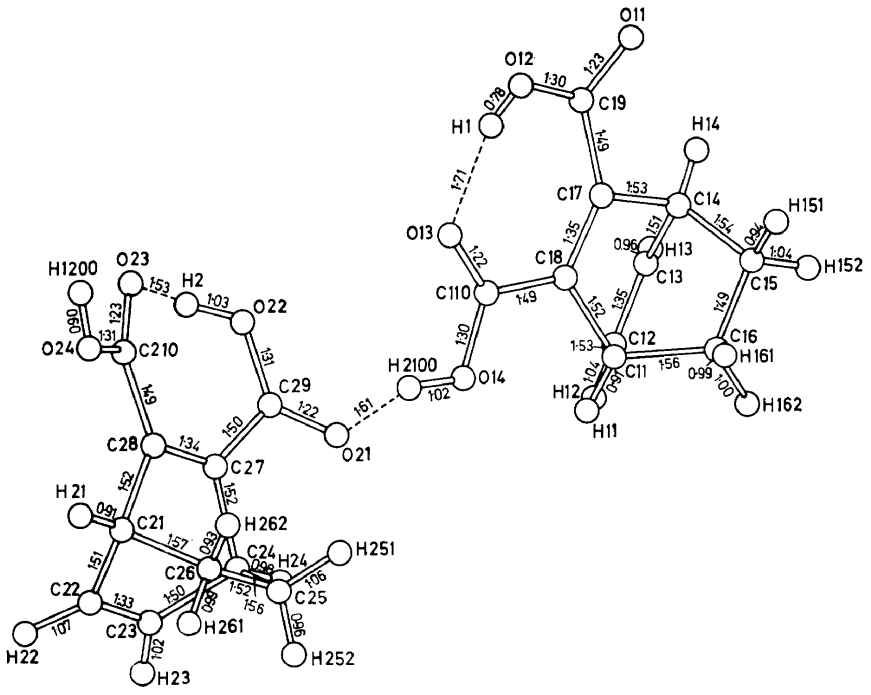

Figure 16. Bicyclo [2.2.2] octadiene (2,5)dicarboxylic acid (2,3). The two molecules in the asymmetric unit; bond lengths are indicated

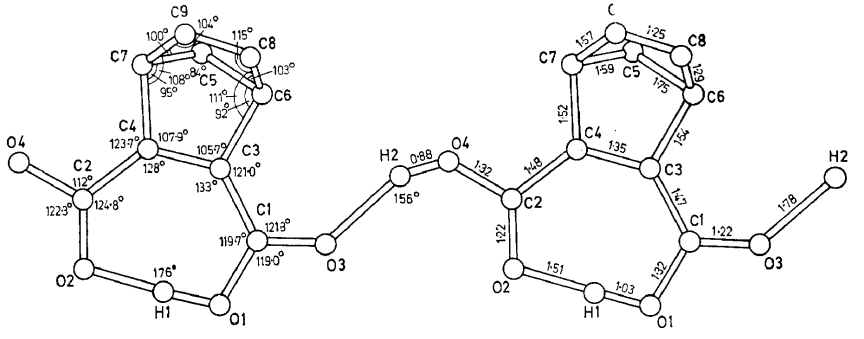

Figure 17. Bicyclo [2.2.1] heptadiene (2,5)dicarboxylic acid (2,3). Two translationally equivalent molecules; bond lengths and angles are indicated

the other hand, the maleic acid conformation will not be influenced by the statistical structure. The bond lengths and the angles agree well with the values found in the bicyclooctadiene-compound. 571 reflections were measured (reflections with $\vartheta > 55°$ were very weak) and a final R-factor of 8·4 per cent was obtained.

A number of structure determinations concerned the conformations of heterocyclic rings containing sulphur atoms. The results will be discussed

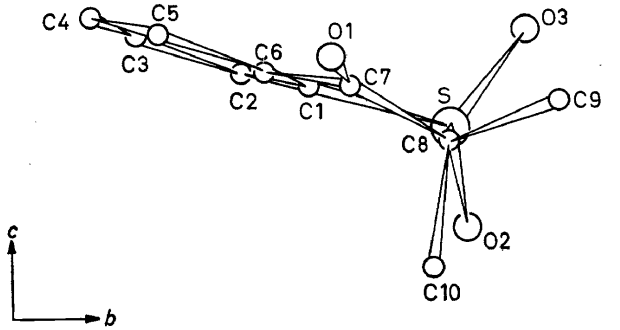

Figure 18. (2,2) Dimethyl-thiaindoxyl (1,1) dioxide. Molecular structure.

together with spectroscopic measurements made by W. Kresze *et al.* elsewhere. I merely wish to make a few comments here concerning the conformation of the rings without describing the crystallographic details. *Figure 18* shows a projection along a direction which is almost in the plane of the benzene ring of (2,2)dimethyl-thiaindoxyl-(1,1)dioxide $C_{10}H_{10}O_3S$ (VII). The atoms in the formula of this compound (VII)—and in formulae

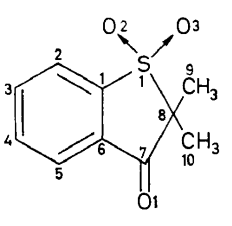

(VII)

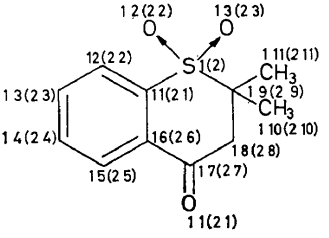

(VIII)

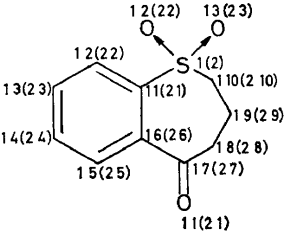

(IX)

(VIII) and (IX) of the two other compounds—have been numbered in the same way as in the figures of the molecular structures. It can be seen from *Figure 18* that the five-membered heterocyclic ring forms a flat half-chair conformation with the quaternary carbon atom slightly displaced from the ring plane. Especially interesting is the molecular structure of (2,2)-dimethyl-thiachromanone(1,1)dioxide $C_{11}H_{12}O_3S$ (VIII). There are two molecules in the asymmetric unit and it can be seen from *Figure 19* that the pronounced half-chair conformations of the six-membered heterocyclic

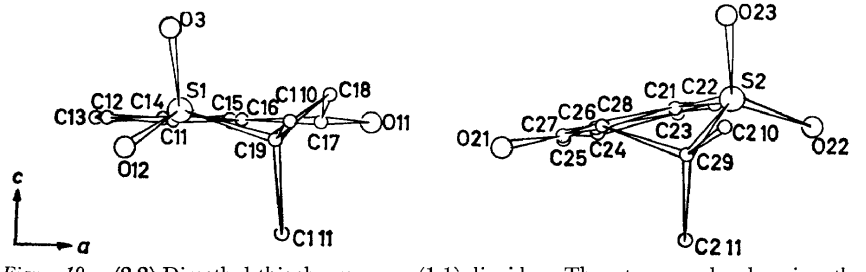

Figure 19. (2,2) Dimethyl-thiachromanone (1,1) dioxide. The two molecules in the asymmetric unit

rings differ in detail appreciably from each other. This is a characteristic example of the influence of the crystal field on the conformation of non-rigid molecules. The structure of the related compound with a seven-membered ring, homothiachromanone(1,1)dioxide $C_{10}H_{10}O_3S$ (IX), turned out to be statistical. The molecular structure is doubled by a non-crystallographic mirror plane. But it can easily be seen from the statistical structure in *Figure 20* that the seven-membered ring has a distorted boat-conformation. The structures of *Figures 18* and *19* have been refined to an R-value of

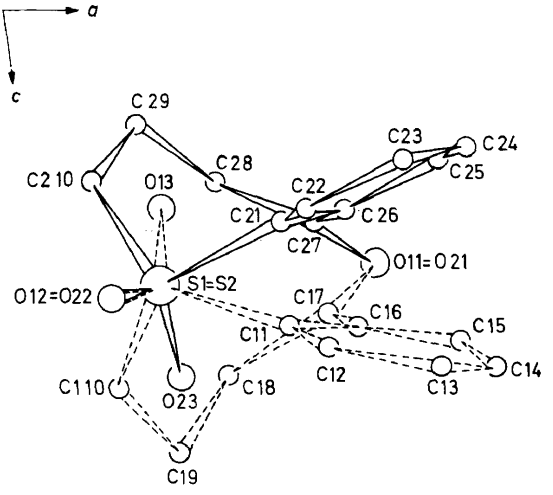

Figure 20. Homothiachromanone(1,1) dioxide. The two molecules that make up the statistical structure

approx. 6 per cent; the statistical structure in *Figure 20* could only be refined to an R-factor of 18 per cent.

I now come to our structural work concerning the chemistry and stereochemistry of organic molecules of biochemical interest. In recent years, we have been especially interested in the chemistry of phorbol. Our results are already published or in print and will, therefore, not be discussed here. But some remarks concerning the methods used might prove useful.

When we started our x-ray work on phorbol, the efforts of the group of chemists collaborating with us (E. Hecker *et al.*) were first directed to the synthesis of a heavy-atom compound suitable for x-ray analysis. But our work was greatly delayed by the fact that the crystals showed disorder, twinning or that the derivative simply did not crystallize at all. In April 1967 we were finally able to report the structure of a neophorbol derivative[11]. This work confirmed the phorbol structure deduced on the basis of chemical work by E. Hecker *et al.*[20]. Somewhat later, another group of workers[21] succeeded in determining the relative configuration of phorbol-20-(5-bromfuroate) by x-ray methods. The interesting point is that their work was also greatly delayed by difficulties in preparing a suitable heavy-atom derivative. Finally we determined the absolute configuration of the phorbol skeleton on the already-mentioned neophorbol derivative[22]. When

we started our work, we had beautiful crystals of the heavy-atom-free compound phorbol itself. At that time we could not determine its structure. The convolution molecule method could not be used because the chemical constitution was not known. Even the later proposal of E. Hecker *et al.*[20] could not help us very much as there were too many stereochemically feasible possibilities for the molecular structure. But some weeks ago we succeeded in determining the crystal structure using a new version of direct methods. If that programme had been available a few years earlier, much annoying and uninteresting chemical work could have been avoided. I should add that these methods have also been used to some extent in the structure analysis of the bicyclo- and sulphur-compounds.

It can easily be shown that the formula derived by Sayre in a simple way by squaring the electron density[23]

$$U_{\vec{h}} \sim \sum_{\vec{h}'} U_{\vec{h}'} U_{\vec{h}-\vec{h}'} \tag{1}$$

can be taken as the computational basis for all direct methods. If one reduces the Sayre sum to one term only, one obtains the triple product relation. But equation (1) does not express the fact that all strong terms in the Sayre sum tend to have the same sign or approximately the same phase. Even in quite complicated organic structures something like ten terms or more obey this rule. The probabilities are so high that a method to determine the signs of the double products individually—the shift product method[24]—even turned out to be slightly inferior to the simple triple product relation, as calculations on various test examples have shown. Our programmes for sign or phase determination are organized in the following way:

1. Approximately 10 per cent of the strongest unitary structure factors are selected.
2. All double product modules which contribute to the (incomplete) Sayre series based on the selected set of reflections are calculated.
3. The origin is fixed by setting the signs (and/or phases) of 3 reflections (4 in the case of projection reflections in an acentric structure).
4. The number of equal signs or equal phases in the Sayre sums is maximised by an iterative procedure.

Let us first discuss point (4). We used different procedures for sign- and for phase-determination. In sign-determination we started from the well-known symbolic addition procedure[25]. This allows one to start with a greater number of reflections. In phase determination the setting of symbols is not possible; the phases are continuous variables. We had to start, therefore, with 3 (or 4) reflections. Our iterative procedure for acentric structures is as follows: We first set a certain high level of probability; and only if one double product in the Sayre sum has a value higher than this level, will the sum be calculated. The first calculations are based on the signs (if projection reflections have been used) or phases of the reflections determining the origin (and of their crystallographic equivalent reflections). Because the probability level is high, many Sayre sums will contain no terms or a single term (triple product relation). Newly developed phases are used immediately for the determination of the next phases in the same

cycle. With the same level of probability a second cycle is calculated. The first phases which at the beginning of the first cycle were only roughly determined now improve. But all other phases are also refined to some extent. Additional cycles follow, until no appreciable change in the phases takes place. Now the level of probability is set lower, new phases are calculated until convergence has again been achieved after a number of cycles. These procedures are repeated until the phases of all chosen reflections are determined. As the programme is fast, a simple extension of this method is possible. One adds two or three additional phases (preferably signs of projection reflections) to the initial set and repeats the phase determination for all permutations of these signs. In effect, this method can be compared to some extent with the symbolic addition process. Again the probability of the right solution will be enhanced, as the initial set is larger. But there is the additional advantage that such a method is a true multi-solution method. The test which we used to differentiate between several solutions is our so-called u-test: The u-factor simply checks how nearly parallel the double product vectors are. The assumption is, therefore, that in the ideal case, all vectors should be parallel. This is wrong, of course, but as a relative measure it means that in the correct set the number of approximately parallel vectors is higher than in another set. This corresponds to our principle that the correct structure is that structure for which the double products in the Sayre sum are most nearly parallel. The u-factor is used in our calculations to check the refinement stage after every cycle and to compare the solutions in the multi-solution process.

I now come to point (3). The determination of the origin is simple in the case of a centrosymmetric structure. In the case of an acentric structure, the origin could, in principle, be set arbitrarily. But in practice, it must be chosen in such a way that the phases of reflections of centrosymmetric projections become signs or obey some special phase rules. Therefore, the normal procedure is to determine the origin by signs or by correctly set phases of projection reflections. We followed this scheme in a number of structure determinations by our method. But there are examples where the strongest reflections are general reflections and where the projection reflections are all weak. This peculiarity appeared, e.g., in the case of phorbol. We therefore used the following procedure: We fixed the origin simply by arbitrarily choosing phases of the three strongest general reflections. This means, of course, that the signs of the projection reflections will become general phases. There are two ways to cope with these difficulties. The first is to rotate the phases of the projection reflections to the nearest signs during the refinement process and to allow the phases of the origin-determining reflections to vary. This means that, in addition to the phases being determined during the process, the origin is shifted to its correct position. This procedure proved to be highly successful in the case of phorbol while a structure determination starting from projection reflections failed. The structure determination based only on the three strongest general reflections led to the correct solution[26]. It should be mentioned that the origin-determining phases were by no means in the neighbourhood of their correct values. To the best of our knowledge, the structure of phorbol is the first structure determined by direct methods, based only on general reflections.

There may be another way to cope with the "wrong origin". It can easily be shown that every structure, even a centrosymmetric structure can be described with reference to a deliberately chosen origin. The symmetry shows up in this case in the form of special phase rules. It would, therefore, be possible to leave the origin fixed and to build the phase rules into the determination of the projection reflections during the phase determination process. This scheme has not yet been tried out.

The combination of phase determination with direct methods or of a phase determination by the heavy-atom technique with phase refinement leads to automatic structure determinations. I am not going to discuss the methods of phase refinement in this paper as this has been done elsewhere[8]. The first structure which was solved by this automatic procedure is that of lumiphorbol[27].

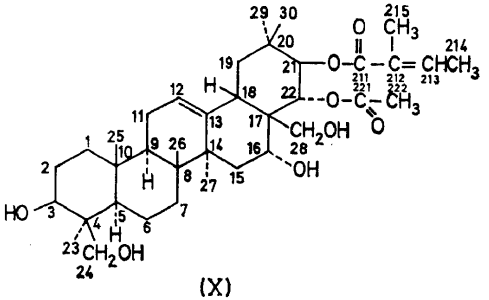

(X)

In the next figures (*Figures 21–24*) I wish to show you the structure of protoaescigenine (21) tiglate (angelate) (22)acetate $C_{37}H_{58}O_8$ (X). The crystallographic data and the molecular structure have already been reported[28].

Figure 21 shows the packing of the molecules in the crystal structure.

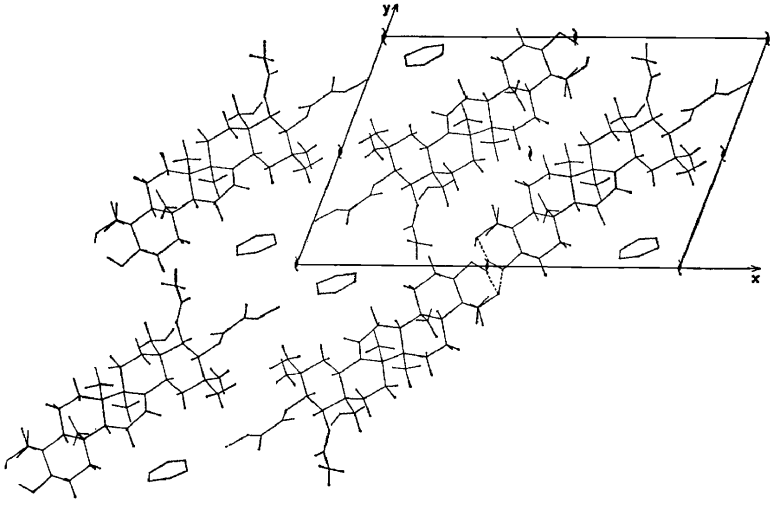

Figure 21. Protoaescigenine (21) tiglate (angelate) (22) acetate. *c*-projection of the crystal structure of the benzene solvate illustrating the packing of the molecules

Around the 2_1-axis at (1/2, 0, z) the molecules are held together by a helical arrangement of alternating intramolecular and intermolecular hydrogen bonds. Near (0, 0, z) there are channels filled with slightly disordered benzene. In contact with this channel is a tiglic acid residue bound to oxygen 21. The final stages of the refinement showed that this is a mixed crystal which contains angelic acid as well as tiglic acid in this position. *Figure 22* shows the interatomic distances (only the tiglic acid has been

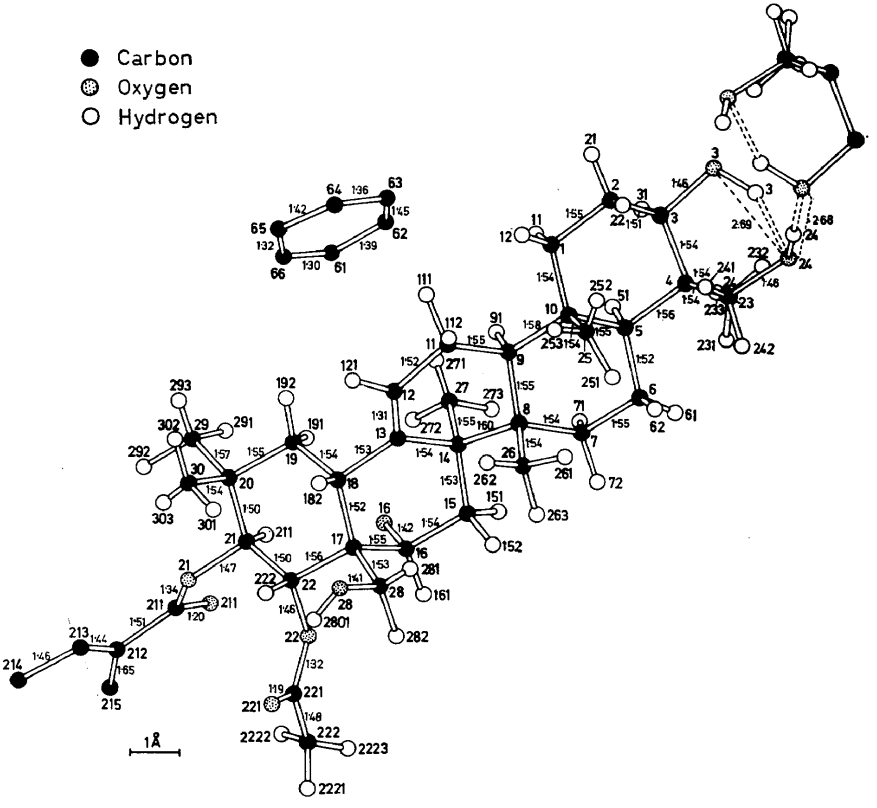

Figure 22. Protoaescigenine (21) tiglate (angelate) (22) acetate. Molecular structure with bond distances

incorporated into the figure) (R = 6·7 per cent). The corresponding Fourier synthesis is shown in *Figure 23*. The low peak heights of the benzene molecule and of several atoms of the ester residue at 0 21 are indicative of disorder in these regions. Fifty hydrogen atoms have been located (all but those of benzene and of the ester at 0 21 and of 0 16) (*Figure 24*).

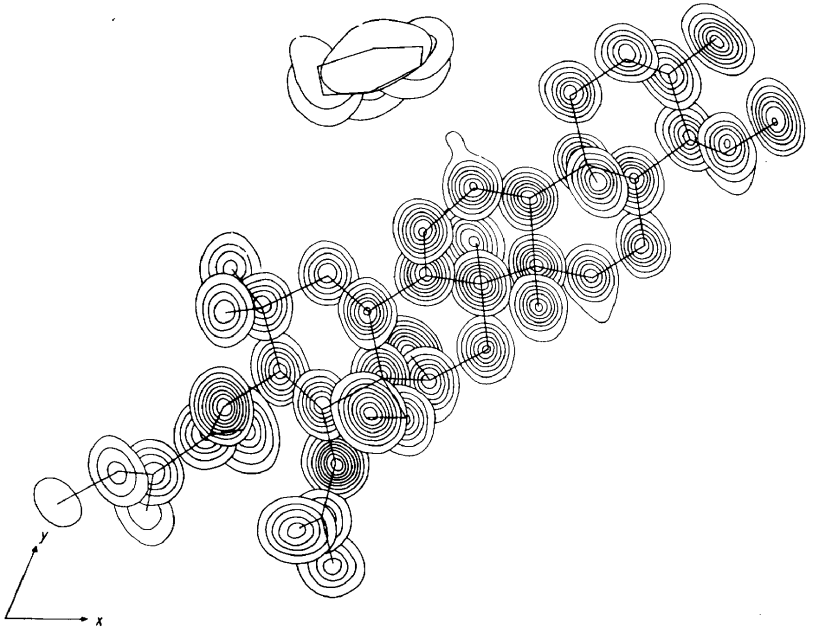

Figure 23. Protoaescigenine (21) tiglate (angelate) (22) acetate. Three-dimensional Fourier synthesis projected along c; contours are at intervals of 1·0 eÅ^{-3} starting with 1·0 eÅ^{-3}

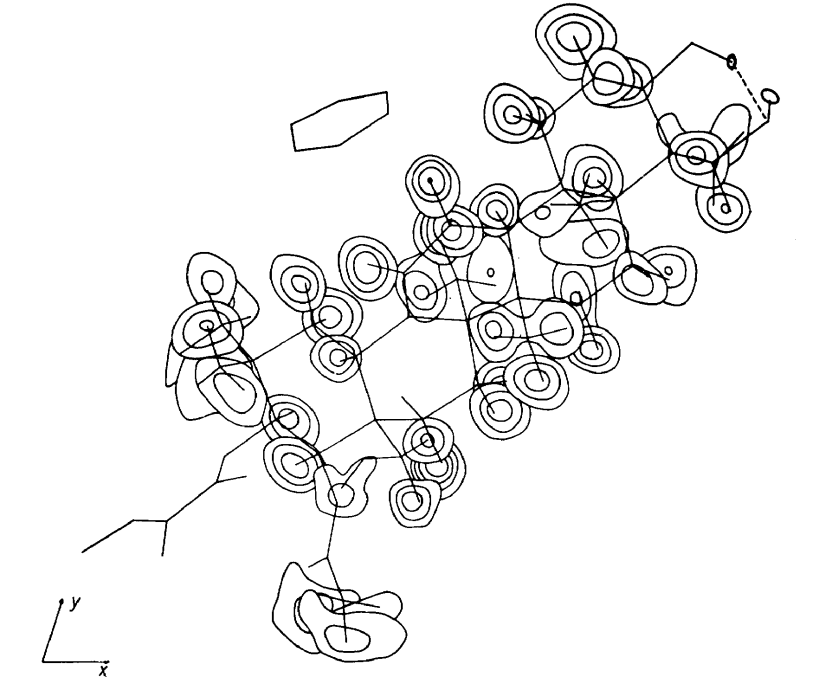

Figure 24. Protoaescigenine (21) tiglate (-angelate) (22) acetate. Difference Fourier synthesis (hydrogen atoms not included in F_c); contours are at interval, of 0·1 eÅ^{-3} starting with 0·1 eÅ^{-3}

Acknowledgement

Our work has been supported by the Deutsche Forschungsgemeinschaft, the Fonds der Chemischen Industrie and the Badische Anilin- und Soda-Fabrik to whom we express our sincere thanks.

References

[1] H. W. Wyckoff *et al.*, *J. Mol. Biol.* **27**, 563 (1967).
[2] W. Hoppe, Abstracts of the International Meeting on Accurate Determination of X-Ray Intensities and Structure Factors, 24–28 June 1968, Cambridge, England. Also *Acta Cryst.*, **A 25**, 1 (1969).
[3] G. Kopfmann and R. Huber. *Acta Cryst.* **A 24**, 348 (1968).
R. Huber and G. Kopfmann. *Acta Cryst.* **A 25**, 143 (1969).
[4] W. Cochran. *Acta Cryst.* **A 25**, 95 (1969).
[5] W. H. Zachariasen. **A 25**, 102 (1969).
[6] S. Hechtfischer, W. Hoppe and K. Zechmeister. Abstracts of the Meeting of the Section für Kristallkunde der Deutschen Mineralogischen Gesellschaft, Bonn, 24–27 April 1967, p. 3.
[7] W. Hoppe. *Z. Elektrochem.* **61**, 1076 (1957).
R. Huber. *Acta Cryst.* **19**, 353 (1965).
[8] W. Hoppe, R. Huber and J. Gassmann. *Acta Cryst.* **16**, A4 (1963).
W. Hoppe and J. Gassmann. *Acta Cryst.* **B 24**, 97 (1968).
[9] J. S. Rollett, this conference.
[10] O. Wimmer. Diplomarbeit TH München 1963.
[11] W. Hoppe *et al. loc. cit.* in ref. 6, p. 53.
[12] e.g. B. F. Hallam and P. L. Pauson. *J. Chem. Soc.* 642 (1958).
[13] e.g. G. Wilkinson in *Advances in the Chemistry of Coordination Compounds* (S. Kirschner Ed.), The Macmillan Co., New York, 1961, p. 50.
S. F. A. Kettle and R. Mason. *J. Organometal. Chem.* **5**, 97 (1966).
[14] I. C. Paul, S. M. Johnson, L. A. Paquette, J. H. Barrett, and R. J. Haluska. *J. Am. Chem. Soc.* **90**, 5023 (1968).
[15] L. Camerer. Dissertation Universität München, 1948.
[16] H. Friedle. Dissertation TH München, 1955.
W. Hoppe, Abstracts of the 3rd International Congress of the International Union of Crystallography, Paris 1954, p. 34.
[17] C. Pascard-Billy. *Bull. Soc. Chim. Fr.* 2282, 2293, 2299 (1962).
[18] H. Brockmann. *Fortschr. Chem. Org. Naturstoffe*, **21**, 121 (1963).
[19] These compounds possess an interesting photochemistry: H. Prinzbach, W. Eberbach and G. Philipossian, *Angew. Chem.* **80**, 910 (1968) and previous papers cited therein.
[20] E. Hecker *et al.*, *Tetrahedron Lett.* 3165 (1967).
[21] R. C. Pettersen *et al.*, *Chem. Commun.* 716 (1967).
[22] W. Hoppe, E. Hecker *et al.*, *Angew. Chem.* **79**, 824 (1967).
[23] D. Sayre. *Acta Cryst.* **5**, 60 (1952).
[24] W. Hoppe, K. Anzenhofer and R. Huber in *Crystallography and Crystal Perfection* (Ed. G. N. Ramachandran), Academic Press, New York, 1963, p. 51.
[25] J. Karle and I. L. Karle. *Acta Cryst.* **21**, 849 (1966).
[26] W. Hoppe, S. Hechtfischer and K. Zechmeister. Abstracts of the Meeting of the Sektion für Kristallkunde in der Deutschen Mineralogischen Gesellschaft, Bern, 3–5 October 1968, p. 23.
[27] E. Hecker, W. Hoppe *et al.*, *Angew Chem.* **80**, 913 (1968).
[28] W. Hoppe, R. Tschesche *et al.*, *Angew. Chem.* **80**, 563 (1968).

Note added in proof

Tetramethylnaphthazarine. New measurements at room temperature and at low temperature have shown after additional refinement that the elliptical hydrogen maximum (*Figure* 12) between O_1 and O_2 moved to a more symmetrical position and became splitted at low temperatures; at the same time the differences of bond length in the pairs ($C_3 - O_1$ 1·284 Å; $C_7 - O_2$ 1·285 Å), ($C_3 - C_4$ 1·411 Å; $C_7 - C_4'$ 1·411 Å) ($C_2 - C_3$ 1·447 Å; $C_6 - C_7$ 1·433 Å) became smaller. Therefore, a statistical structure can no longer be excluded.